Designing sequence-defined biomimetic peptoids for self-assembly

Renyu Zheng

A thesis

submitted in partial fulfillment of the requirements for the degree of

Master of Science in Chemical Engineering

University of Washington

2021

Committee:

Chun-long Chen

Lilo Pozzo

Program Authorized to Offer Degree:

Chemical Engineering

University of Washington

Abstract

Designing sequence-defined biomimetic peptoids for self-assembly

Renyu Zheng

Chair of the Supervisory Committee:

Chun-long Chen

Chemical Engineering

Nanostructured inorganic materials provide unique properties in various fields, including plasmonics, catalysis, sensing, and optics compared with their bulk counterparts. Inspired by sophisticated nanostructures created by living organisms using sequence-defined biomolecules, scientists are developing various biomimetic approaches to control inorganic material formation. In this work, we designed a series of sequence-defined peptoids. We demonstrated their self-assembly into nanosheets, nanotubes, and nanofibers, potentially used as templates for inorganic material formation. We presented the morphologies of these self-assembled structures could be controlled through the variation in peptoid building blocks. The knowledge learned here will benefit our future use of these peptoid materials as templates to induce the formation of inorganic materials various morphologies.

Acknowledgments

The author expresses sincere appreciation for Dr. Chun-long Chen's guidance and encouragement. The authors would also like to show great thanks to Dr. Shuai Zhang, who provided detailed in-person guidance in characterization and plenty of suggestions for result discussion. Besides, the author also wants to thank Mr. Wenchao Yang for peptoid synthesis, Mr. Peng Mu for some AFM images and Dr. Mingfei Zhao for molecular simulation. At last, great appreciation to the CSSAS for providing such an interdisciplinary platform for scientific collaboration

Contents

1. Introduction

1.1 Introduction to peptoids

In nature, peptides and proteins are crucial in the formation of varieties of hierarchically structured functional materials. They control the nucleation, growth, and organization of mineral crystals by either acting as soluble surfactants or serving as highly ordered self-assembled scaffolds[1]. Inspired by nature, various biomimetic approaches have been developed by using short synthetic peptides or de novo proteins to induce inorganic crystal formation and organization in the absence of any biological contexts[2]. However, the complexity of peptide folding makes the peptide-controlled inorganic crystal formation process hard to understand and predict. For example, a rapid change in peptide secondary structure observed during peptide-controlled SiO_2 formation complicated our understanding of the roles that peptide sequences and side-chain chemistry play during the inorganic crystal formation[3].

Peptoids (poly-N-substituted glycine) are one type of unique sequence-defined synthetic polymers that combines the merits of both biomolecules (biocompatibility and sequence programmability) and polymers (high stability and easy to synthesize) [4]. With the side groups moved from α-carbon to nitrogen atom as shown in Fig. 1, peptoids lack hydrogen bond donors, eliminating the formation of intermolecular backbone hydrogen bonds. This reduction in structural complexity makes the properties of peptoids predominantly determined by their side-chain chemistry, simplifying their design and engineering. Peptoids can be easily synthesized through a sub-monomer method, as shown in Fig.1[5]. Each cycle of monomer addition consists

of two steps: one acylation reaction of amine by bromoacetic acid and one nucleophilic substitution of halogen by primary amines, where various side chemistry can be introduced.

On the one hand, recent studies have reported the peptoid-controlled synthesis of metal nanoparticles where peptoids were used as surfactant mediators [6-8]. On the other hand, peptoids can also self-assemble to hierarchical nanostructures like tubes or sheets [9, 10]as scaffolds for inorganic material assemble or grow in specific spatial arrangements[11, 12]. In the latter approach, besides conjugating inorganic materials on peptoid systems, controlling the peptoid self-assembly to different morphologies is crucial to peptoid-templated material formation. In this thesis, we mainly focus on designing different peptoid sequences to realize various nanostructures, including tubes, sheets, and helical fibers. By systematically studying the relationship between peptoid sequence and self-assembled structures, we have expanded the library of peptoid-assembled nanostructures as templates for inorganic material growth and further explained the formation mechanism for these assemblies.

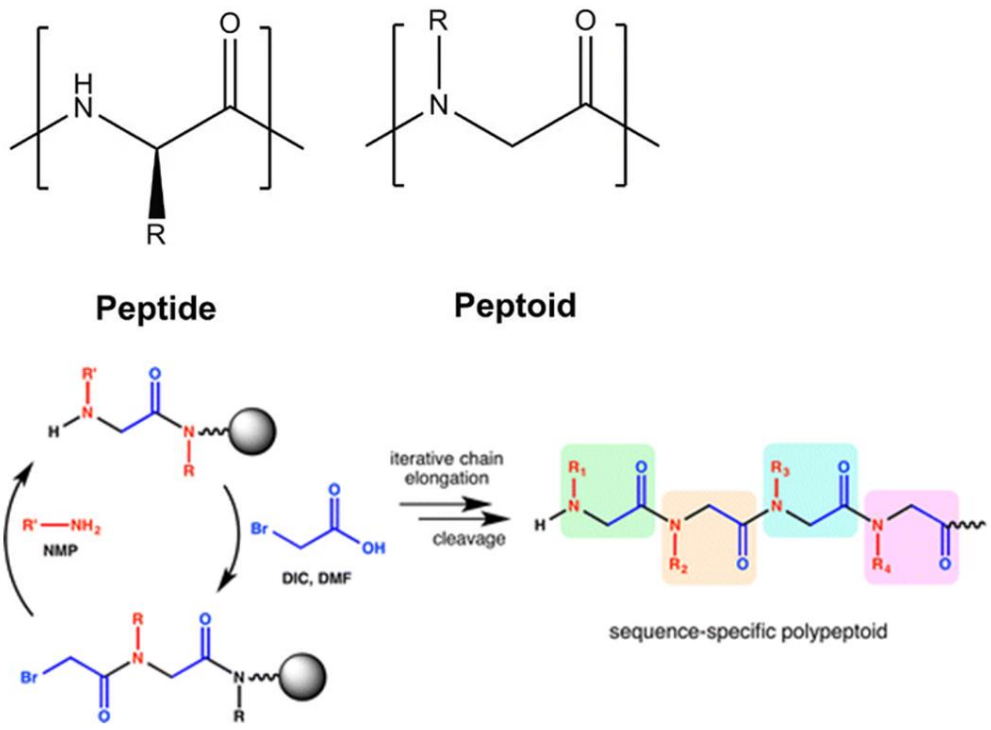

Fig.1 The structure of peptides and peptoids and the schematic of peptoid synthesis. Side groups in peptides are moved from α-carbon to nitrogen atom to eliminate the secondary structures result from the amide hydrogen bond in peptides. Peptoids can be synthesized through a sub-monomer method, which contains an alternative coupling reaction between amine and bromoacetic acid and a substitute reaction to introduce desired side group and elongate the peptoid chain[13]

1.2 Peptoid self-assembly to hierarchical structures

Living organisms widely adopt molecular self-assembly to build well-defined functional structures, including cell membranes[14], cytoskeletal filaments[15], collagens[16], and amyloid fibrils[17]. In biomimetic studies, scientists endeavor to understand the construction philosophy adopted by living organisms and design synthetic molecules to build functional structures. Plenty of work reported using natural biomolecules like peptides[2] and nucleotides[18] to construct hierarchical structures. Compared with these biomolecules, peptoids offer a highly programmable organic building block similar to peptides that exhibit large side-chain diversity for multifunctional material synthesis. Besides, with the lack of backbone hydrogen, they are highly thermally and chemically stable and provide unique simplification for controlling self-assembly since the side chemistry predominates their properties. Taking advantage of the controllability of peptoid side chemistry, scientists can synthesize a range of self-assembling structures with atomic precision and understand how side chemistry or sequence affects the structure and hierarchy of different peptoid-based materials.

Our group has reported using amphiphilic peptoids with hydrophilic carboxyl groups and hydrophobic aromatic groups to self-assemble into either 2D nanomembranes[10] or 1D nanotubes[9]. The controlled assembly of sheets or tubes can be achieved by tuning the hydrophobic building submonomers, as shown in Fig. 2. We also demonstrated that hydrophobic interactions play a significant role during the self-assembly of hierarchical structures by adjusting the number of hydrophobic units in peptoid design[10]. However, the specific role of these building blocks, how different morphologies can be controlled through the variation of one carbon remains elusive, and some other common self-assembled structures observed in peptide assemblies, like helical fibrils, are rarely reported for peptoid in peptoid assembly. In this work, we designed peptoids with various hydrophobic domains with alternative N-[2-(4-bromophenyl) ethyl(or methyl)] glycines (Pep-Br-C2 and Pep-Br-C1) to further understand the formation mechanism of these self-assemblies. We also design peptoids with only one carboxyl group to investigate the role of hydrophilic domain and see if the peptoids self-assembly will adopt an alternative pathway as reported[19], or even a different final structure.

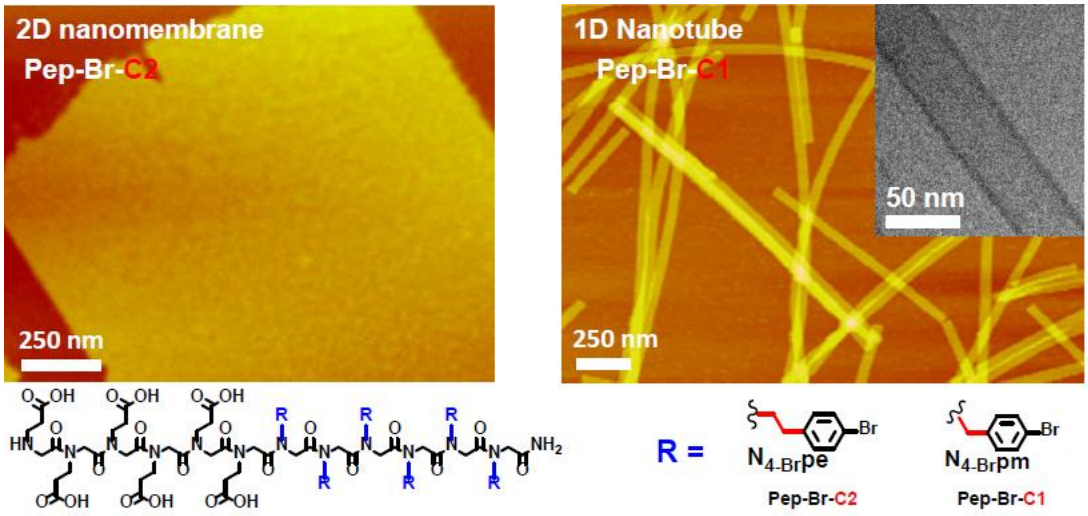

Fig. 2 Controlled self-assembly of peptoid nanomembranes and nanotubes by tuning hydrophobic building blocks. Six hydrophilic N-(2-carboxyethyl) glycine groups are used to mimic the polar groups in lipids and stabilize the self-assembly

1.3 Peptoid-directed hierarchical assembly of functional objects

Based on our recent success in the self-assembly of peptoids into highly crystalline nanotubes or nanosheets, we also demonstrated the use of hierarchical peptoid assembly to organize functional groups. These peptoid-based hierarchical materials can act as platforms to assemble quantum dots and clusters[12], building blocks for hybrid inorganic-organic materials[20], and templates for metal nanoparticle growth[11]. For example, in our CSSAS team (Center for Science of Synthesis Across Scales), Madison et al. [12]conjugated maleimide groups to the end of reported sheet- and tube-forming peptoid sequences and synthesized peptoid sheets and tubes with maleimide groups on their surface. (Fig. 3a) The maleimide moieties can react with cysteine-capped CdSe quantum dots (QD) through thiol-maleimide reaction and induce the formation of a hybrid peptoid-QD system(Fig. 3 b-d). Besides, by replacing the carboxyl groups with methoxy ether groups, the authors could also control the QD density as a function of maleimide concentration. In another example, Ma et al. used solid-binding proteins to conjugate with maleimide-containing peptoid sheets. They then used these functional sheets as scaffolds for controlling the organization of SiO_2 inorganic nanoparticles. In this case, the interaction of silica-binding protein Car9 with silica nanoparticles resulted in forming a multilayered material composed of alternating peptoid, protein, and organic layers [20]. (Fig. 4a). In a third example,

Merril et al. [11] used amine groups modified peptoid sheets and fibers as scaffolds to direct the formation of Pd nanomaterials with a 2D network or 1D chain-like structures (Fig. 4b).

These previous studies have proved the potential of self-assembled peptoid nanostructures as templates for controlling inorganic crystal formation, [21]. However, peptoid-controlled inorganic crystal formation is still in its infancy, and further investigation on peptoid assembly is needed to develop a predictive understanding of their impact in the construction of hierarchical materials. For example, while controlled synthesis of peptoid nanosheets and nanotubes has been previously reported, their formation mechanisms and the correlation between sheets and tubes remain unclear. Therefore, this thesis mainly focuses on controlling peptoid self-assemblies to different morphologies via molecular design (different peptoid structures) and experimental conditions (like pH change). In addition, by the systematic comparison between peptoid molecular structures and corresponding assemblies, we are clarifying the role of different building blocks in a single molecule to direct hierarchical assemblies.

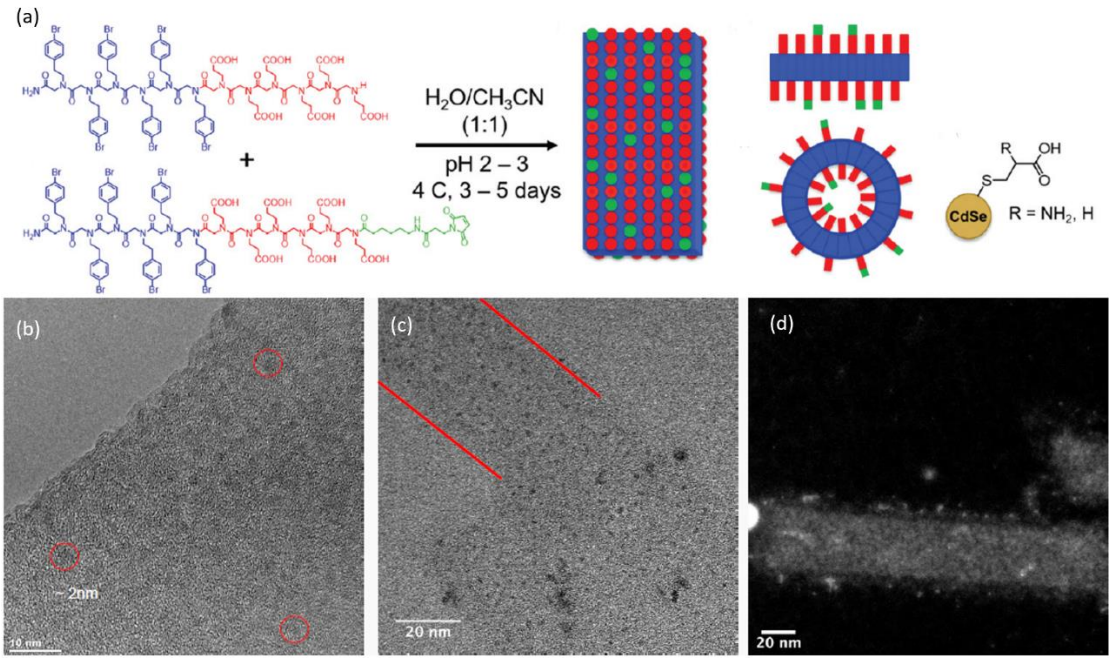

Fig.3 a) Schematic of synthesis of maleimide-containing peptoid sheets, and conjugation with cysteine-capped QDs. Peptoids modified with maleimide end groups co-assemble with the same peptoid sequence without the modification to form template tubes or sheets. (Blue: Hydrophobic groups, Red: Hydrophilic groups, Green: Reactive maleimide end group). CdSe growth on assemblies is via thiol-maleimide reaction b)-d) TEM images of CdSe materials on peptoid sheets and tubes. b. Alignment of CdSe magic size clusters parallel to the tube edge. c. QDs growth with a preference on nanotubes. d. STEM image of QDs growth along the edges of peptoid nanotubes.

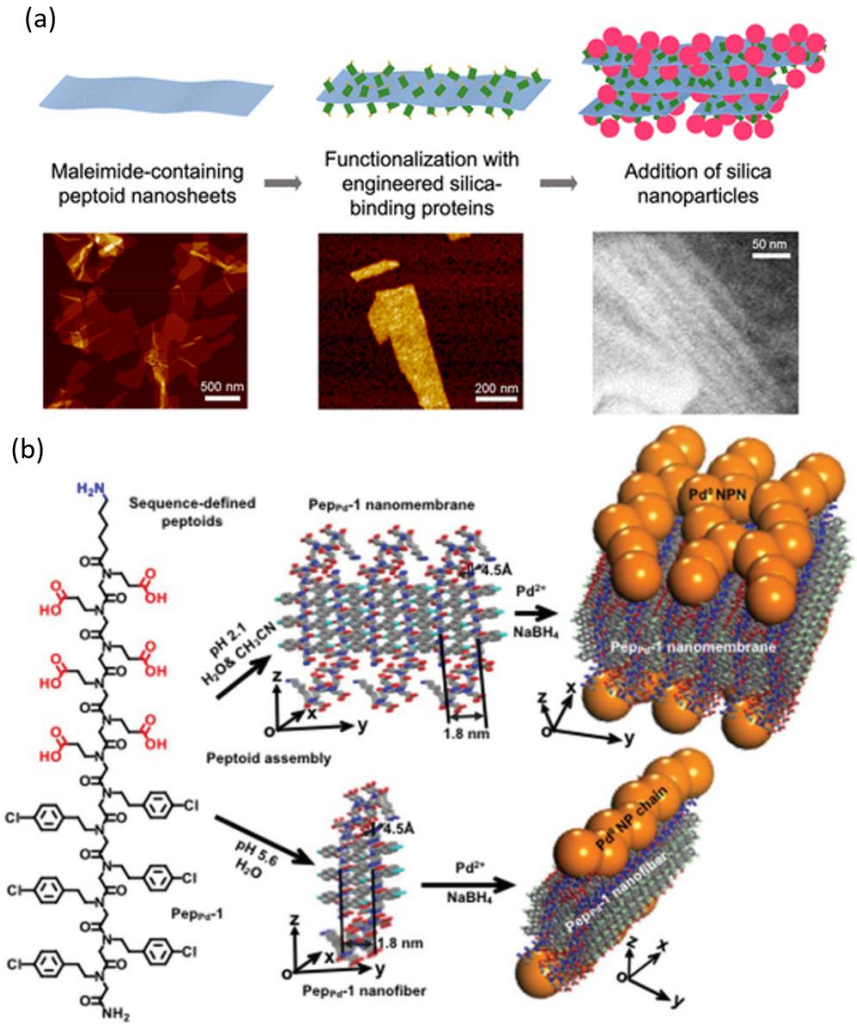

Fig. 4 Schematic of a) Peptoid conjugated with silica-binding proteins to induce hierarchical inorganic-organic multilayers. b) Self-assembled peptoid membranes and fibers as scaffolds for PdNP growth

2. Experiment methods

2.1 Materials

N, N'-diisopropyl carbodiimide, bromoacetic acid, and trifluoroacetic acid (TFA) were purchased from Chem-Impex International, Inc and used as received. 4-Bromobenzylamine was purchased from Oakwood Products, Inc and used as received. Rhodamine B, N, N-diisopropylethylamine (DIPEA), triisopropylsilane, and dopamine hydrochloride were purchased from Sigma-Aldrich and used as received. All other amine submonomers and other reagents are obtained from commercial sources and used without further purification. MilliQ water at 18MΩ cm was used for all experiments.

2.2 Synthesis and purification of peptoids

All the peptoids were synthesized by Chen group members at PNNL following the reported protocol [9, 10]. Some peptoids were synthesized on a commercial Aapptec Apex 396 robotic synthesizer using a solid-phase submonomer cycle as described previously[5, 10]. Rink amide resin (0.09 mmol) was used to generate C-terminal amide peptoids. In this method, the Fmoc group on the resin was deprotected by adding 2mL of 20% (v/v) 4-methylpiperidine/N, N-dimethylformamide (DMF), agitating for 20 min, draining, and washing with DMF. All DMF washes consisted of the addition of 1.5 mL of DMF, followed by agitation for 1 min (repeated five times). An acylation reaction was then performed on the amino resin by adding 1.6 mL of

0.6M bromoacetic acid in DMF, followed by 0.35 mL of 50% (v/v) N, N-diisopropyl carbodiimide (DIC)/DMF. The mixture was agitated for 30 minutes at room temperature, drained, and washed with DMF five times. Nucleophilic displacement of the bromide with various primary amines occurred by a 1.6 mL addition of the primary amine monomer as a 0.6M solution in N-methyl-2-pyrrolidone (NMP), followed by agitation for 60 min at room temperature. The monomer solution was drained from the resin, and the resin was washed with DMF five times. The acylation and displacement steps were repeated until a polypeptoid of the desired length was synthesized.

The final crude product was cleaved from the resin by the addition of 95% trifluoroacetic acid (TFA) in water, which was then evaporated off under a stream of N_2 gas. Finally, crude peptoids were dissolved in H_2O/CH_3CN (v/v = 1:1) for HPLC purification. The crude products were purified by reverse-phase HPLC on an XBridge Prep C18 10 µm OBDTM (10 µm,19mm × 100 mm), using an adaptable gradient of acetonitrile in H_2O with 0.1% TFA over 15 min. Purified peptoids were analyzed using Waters ACQUITY reverse phase UPLC (corresponding gradient at 0.4 mL/min over 7 min at 40 °C with an ACQUITYBEH C18, 1.7 µm, 2.1 mm× 50mm column) that was connected with a Waters SQD2 mass spectrometry system. The final peptoid product was lyophilized at least twice from its solution in a mixture (v/v = 1:1) of water and acetonitrile. The peptoid powder was finally divided into small portions (2.0×10^{-6} mol) and stored at 4°C.

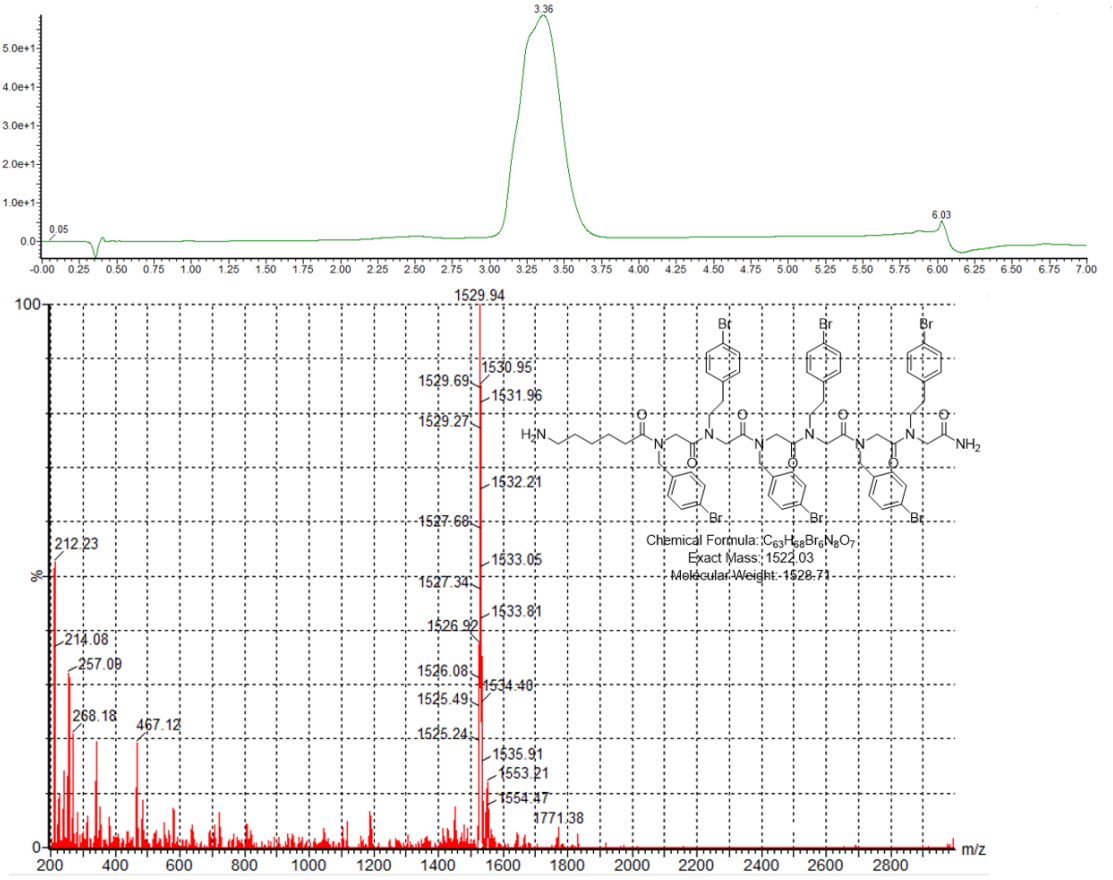

Fig. 5 UPLC-MS data of peptoid.

2.3 Self-assembly of peptoids

1 µmol of lyophilized peptoid powders were dissolved in 95% TFA solution, evaporated, and dissolved in 200 µL of water and acetonitrile (v/v = 1:1) mixture to make 5.0mM clear solution. The mixture was then put in the 4 °C refrigerator for slow evaporation. About 2 or 3 days later, gel-like materials or precipitates were obtained. For stability test with different pH, take 10uL of

the gel-like solution and adjust the solution pH by adding sodium hydroxide solution. The solution was still incubating at 4 °C for time-dependent study.

2.4 Atomic Force Microscopy

Ex-situ AFM tests (in the air) were performed on Bruker ICON using PeakForce Quantitative Nanomechanics mode. 1μL drop of the gel-like solution was diluted with 40uL of deionized water and placed onto a freshly cleaved mica substrate for 10 min. Then use Kimwipe to absorb the excess solution and bring the sample to test. For some solutions assembled to white precipitates instead of gel-like materials, take the precipitate and wash with deionized water three times. Dilute the suspension, drop it onto the mica surface and let it dry in the air without any treatment.

3. Results and discussion

3.1 Design of peptoids

As a biomimetic study, inspired by the amphiphilic molecules that can assemble to hierarchical structures like lipids, we designed a series of amphiphilic peptoids that contain two sub-blocks, respectively, N-[2-(4-chloro-/bromo- phenyl) ethyl(or methyl)] glycines (N4-Br,Clpe/pm) for hydrophobic building block, and 6-aminohexanoic acid (Nc6), N-(2-carboxyethyl) glycine (Nce) and glycolic acid (Dig, named after the peptoid treated with diglycolic acid) as hydrophilic building blocks. Aromatic hydrophobic groups were chosen because they mimicked the nonpolar hydrophobic tail in lipids and are reported to strengthen the self-assembled structure through π-π interactions [22]. Hydrophilic groups were introduced to mimic the polar lipid head groups, where Nce/Dig groups are reported hydrophilic building blocks, and Nc6 may play as both polar group and metal-binding groups. In this thesis, my goal is to synthesize self-assembled peptoid nanostructures and to control their morphologies by variation in building blocks. By establishing a relationship of peptoid molecular structures and corresponding self-assemblies, various candidates can induce inorganic material formation.

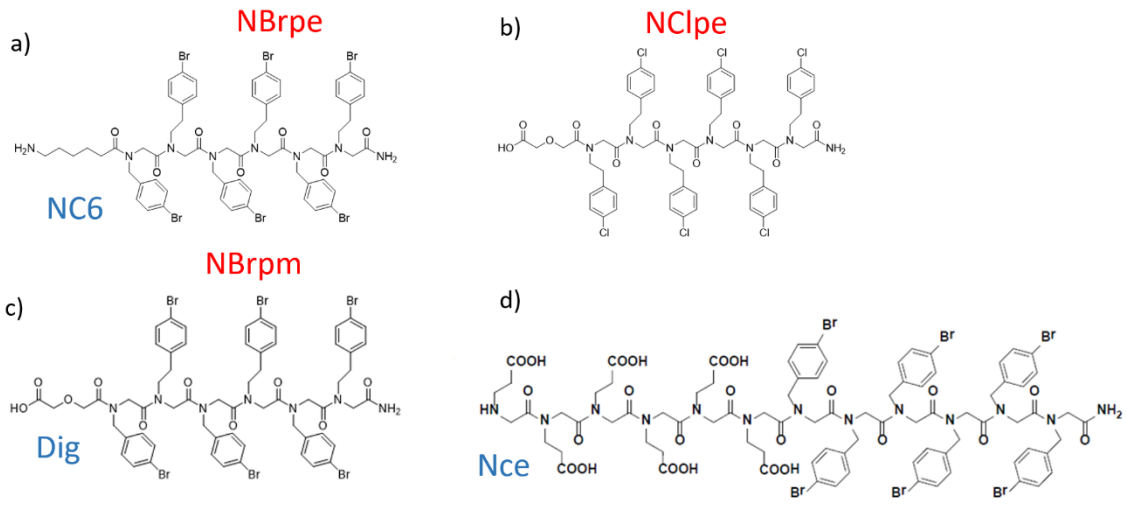

Fig. 6 Structures of peptoids: a) (NBrpeNBrpm)3Nc6; b) NClpe6Dig c) (NBrpeNBrpm)3Dig; d) NBrpm5Nce6. Hydrophobic building units marked as red: N-[2-(4-bromophenyl) ethyl] glycine (NBrpe); N-[2-(4-bromophenyl) methyl] glycine (NBrpm); N-[2-(4-chlorophenyl) ethyl] glycine (NClpe). Polar groups marked as blue: N-(2-carboxyethyl) glycine (Nce), 6-aminohexanoic acid (Nc6) and one carboxyl group (Dig)

3.2 Tuning peptoid self-assembly by hydrophobic group

Peptoid self-assembly is triggered through an evaporation-induced crystallization process. Peptoid solution, with a concentration of 5mM in acetonitrile and H_2O (v/v: 50/50), was put in 4°C for slow evaporation. After 2-3 days, gel-like materials containing a large amount of crystalline self-assembled structures formed and characterized by atomic force microscopy (AFM).

In our previous work[11], we demonstrated that the amino hexanoic acid (Nc6) end group could induce templated PdNP formation through the binding of Pd with the amine group. And we also showed that for peptoid self-assembly, hydrophobic interaction plays the dominant role

in determining the final morphologies, while hydrophilic or polar domain help to stabilize the assembled structures and may result in a different pathway for the formation[19]. Since the Nc6 group is also polar, herein we investigated three peptoids: NBrpe6Nc6, NBrpm6Nc6, and (NBrpeNBrpm)3Nc6, to demonstrate: 1) Nc6 group, which has the potential to induce nanoparticle formation through their high metal-binding affinity, can also act as a polar group to trigger the peptoid self-assembly as Nce groups. 2) Controlled synthesis of nanotubes or nanosheets is also available in this system through the variation of hydrophobic building block, following the same rule as reported[9, 10]. 3) The peptoid with asymmetric hydrophobic domain (NBrpeNBrpm3Nc6) can assemble to a special nanosheet with stripes. Detailed analysis on the stripes help to reveal the molecular packing of the peptoids.

Dry-condition AFM (performed in air) was used to characterize the self-assembled structures. As shown in Fig. 1a, NBrpe6Nc6 can assemble into nanosheets with a height of around 3nm. Overlapping sheets indicated their free-standing state in the solution and overlapped during sample preparation. In Fig. 1b, NBrpm6Nc6 can assemble into nanotubes with a height around 6nm. Dimensions of the tubes and sheets produced from the peptoids with Nc6 group are like the ones we reported, respectively[9, 10], which demonstrated the variation in the hydrophobic domain, from NBrpe to NBrpm, can also control the assembly morphologies from sheets to tubes in peptoids with Nc6 end group.

The controlled formation of sheets or tubes via the switch in hydrophobic building units triggered the design of peptoid with alternative NBrpe and NBrpm groups for further investigation on the molecular packing and formation mechanism for the self-assembly process. As a result, the peptoid with the asymmetric hydrophobic domain can assemble into nanosheets with stripes. The heights of the sheets are 2-3 nm, which is the similar as the one from NBrpe6Nc6, where some stripes grow at the nanosheet surfaces to create protrudes with the

height at around 1nm. The stripes on the sheets create more possibilities for inorganic material growth. For example, the uneven sheets have a larger surface area and more excellent capability to carry inorganic materials. Besides, the well-aligned stripes on the sheet may induce in-situ growth of metal nanoparticles on it and create a unique 3D arrangement of nanoparticles. For example, Merrill et al. [11] reported that PdNP with chain-like arrangement performed significantly enhanced catalytical activity for olefin hydrogenation compared with disordered NP networks on 2D materials. Therefore, well-aligned NP chains on a 2D material may have greater catalytical performance due to a more efficient display. In addition, amine groups are also reported as functional moieties for the in-situ growth of gold and silver nanoparticles[23, 24]. Peptoid nanosheet with stripes also has the potential to induce AuNP or AgNP to arrange in a chain-like manner, which are reported to have enhanced plasmonic properties for potential application in photonic, magnetic, and electronic devices[25, 26].

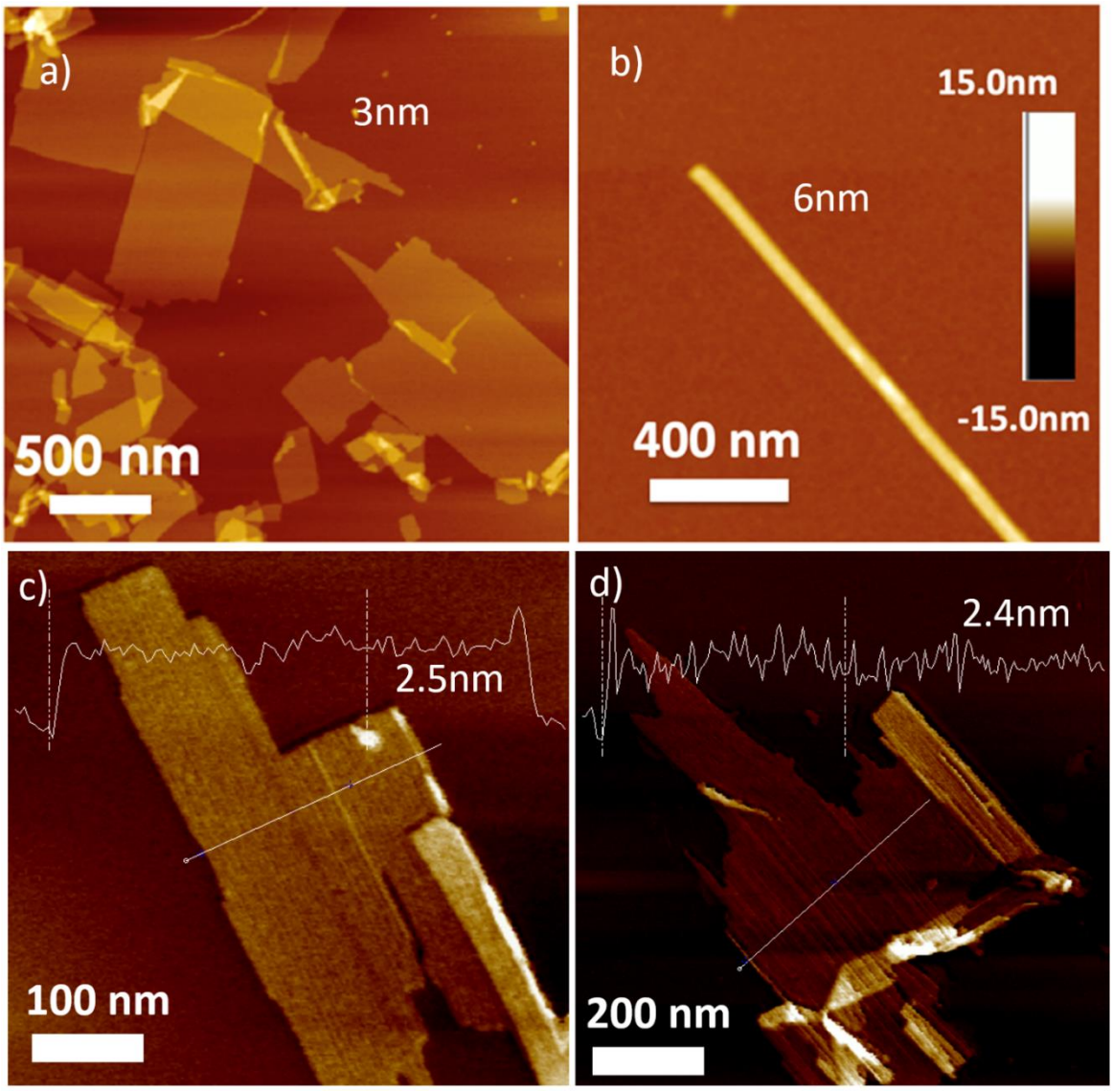

Fig. 7 AFM images of nanostructures assembled from peptoids with Nc6 hydrophilic group and NBrpe/NBrpm hydrophobic groups: a) Nanosheet assembled from peptoid NBrpe6Nc6. (From Peng Mu) Freestanding nanosheets with a height around 3nm are the same as the previously reported sheets[10]. b) Nanotubes assembled from peptoid NBrpm6Nc6. Tubes with heights around 6nm are the same as previously reported tubes[9]. c),d) Nanosheets with stripes grown along the longitudinal direction assembled from peptoid (NBrpeNBrpm)3Nc6, with the height

around 2.5nm. Heights along the section is provided to demonstrate the uneven surface with stripes.

High-resolution AFM was performed to further investigate the stripe structures in the nanosheet assembled from peptoids with two different hydrophobic building units. Well-aligned stripes along the y-direction in Fig.7c-d and Fig.8 indicate the anisotropic growth of peptoid nanosheets as reported[10]. Peptoid molecules are packed and assembled into sheets faster along the y-direction than the x-direction. Therefore, the molecular packing model for the sheet with stripes is like the model proposed for NClpe6Nce6 as Fig. 8b: peptoid molecules align in the y-direction with stronger hydrophobic interactions than in x-direction, but exchanges in both directions are strong enough to form the sheet structure.

For the peptoids with alternative hydrophobic submonomers, two possible packings in the x-direction are possible. The NBrpe and NBrpm groups may pack with each other respectively (denoted as MMEE), alternatively (denoted as MEME), or randomly. The three packing models would lead to different backbone distance in x-direction since the packing of NBrpm groups results in a distance of 1.67nm as reported in nanotubes[9]. Therefore, the distance between the stripes grown on the sheet surface may provide information about the molecular packing. As shown in Fig. 8a, the distance between stripes was measured at 1.8nm homogeneously, satisfying the MEME packing. We also performed a molecular dynamic simulation to understand the molecular structure of the sheets. As shown in Fig. 8c, the MEME packing is a thermodynamically stable state in the system, where the backbone distance in the x-direction is also 1.8 nm. The peptoid seemed to adopt the homogeneous MEME packing at the current stage, but the confirmation requires XRD analysis in the future.

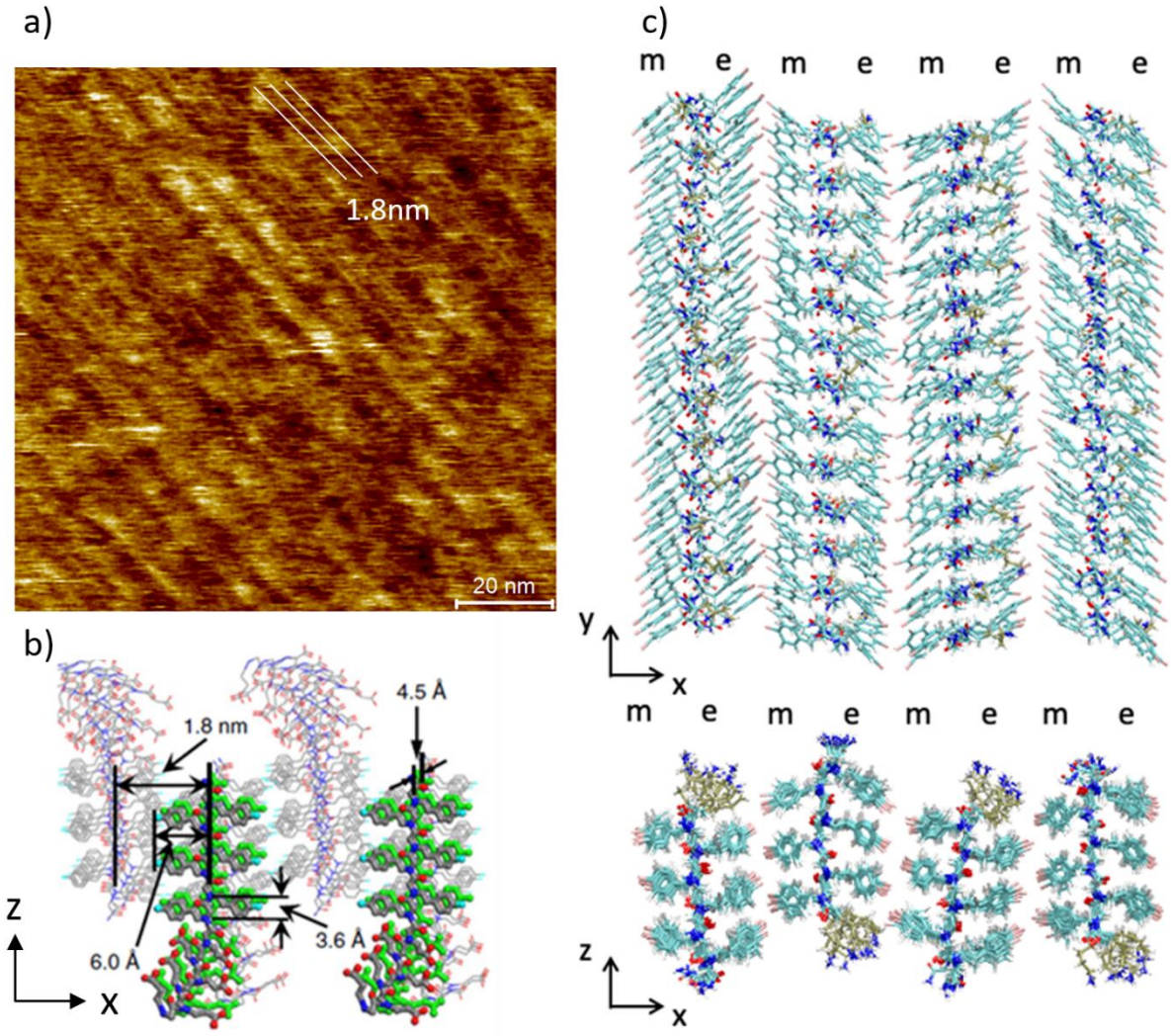

Fig.8: a) High-resolution image of peptoid sheet assembled from (NBrpeNBrpm)3Nc6. Noticeable stripes are shown here. The distance between adjacent stripes is 1.8nm. b) Reported molecular packing model for peptoid sheet assembled from NClpe6Nce6. Backbone distance is 4.5Å along y-direction and 1.8nm along the x-direction, which satisfies the stripe distances. c) Molecular simulation that shows alternative packed NBrpm(M) and NBrpe(E) along y-direction is

a thermodynamically stable crystalline packing. The backbone distance along the x-direction is also 1.8nm.

3.3 Tuning peptoid self-assembly by varying hydrophilic group

In addition to control the self-assembly morphologies through variation in hydrophobic groups, we also further investigated the role of the hydrophilic domain. According to reported peptoid self-assembly models for NClpe6Nce6(Fig. 8b), large hydrophilic must be floppy to minimize the exposure of hydrophobic domain in water. The floppy block creates an additional challenge for molecular simulation since it brings extra complexity to this system. To simplify the structure of amphiphilic peptoid self-assemblies, we designed peptoids with only one carboxyl group as the hydrophilic tail (denoted as Dig). In addition, different morphologies are expected for this variation as well.

As a result, the peptoid NClpe6Dig can still assemble into nanosheets with the height of 3.5nm (Fig. 9a), similar to the reported sheet assembled from peptoid NClpe6Nce6 and NClpe6Nce3 that has 6 and 3 carboxyl groups, respectively. However, the peptoid with three hydrophobic NClpe units could not assemble into sheets [10]. Comparison between the sequences demonstrated the importance of hydrophobic interaction in peptoid self-assembly, while only one carboxyl group can still play as the hydrophilic domain and stabilize the sheets.

Surprisingly, when the Dig end group is connected to the asymmetric hydrophobic group (NBrpeNBrpm)3 as described above, the peptoids assembled to helical fibers instead of tubes or sheets, as shown in Fig. 9b. The helical fibers had a similar period around 80nm, and the heights of 10-15 nm varied for crest and trough(Fig. 9c). Both left-handed and right-handed helices were observed. The successful synthesis of helical fibers expanded the possible self-assembled

structures from peptoids. In addition, helical assemblies from peptides are reported as templates to induce 3D superstructures of nanoparticles in chiral architectures [27-29]. Their intrinsic asymmetry of nanoparticles grown on helical templates gives rise to various interesting properties, including plasmonic chiroptical activity in the visible spectrum. They hold immense promise as chiroptical sensors and as components of optical metamaterials[30].

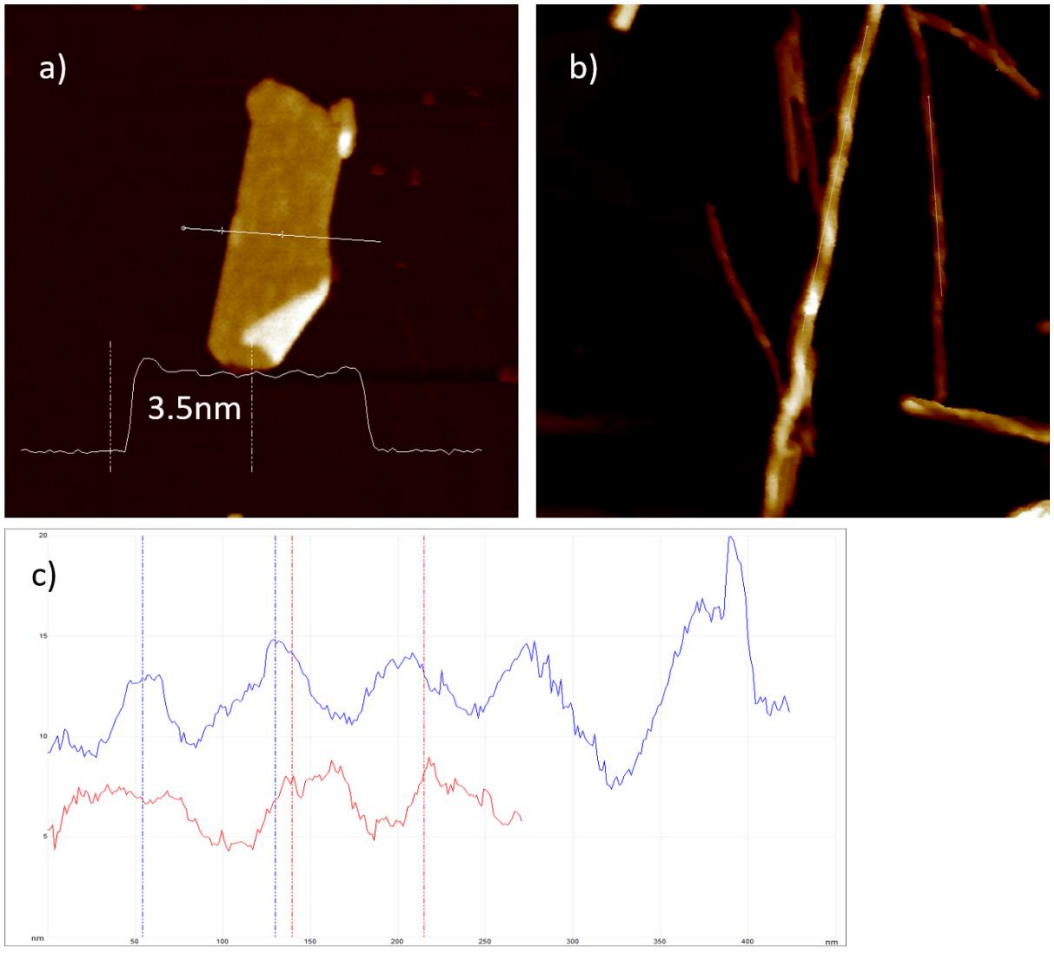

Fig. 9: a) Nanosheet assembled from NClpe6Dig, with the height of 3.5nm, same as the sheet assembled from NClpe6Nce6. b) Helical fibers assembled from (NBrpeNBrpm)3Dig. Helical

structures did not show a preference for one handiness. The period of the helices is shown in c), at around 80nm. The height of the fibers are varied between 10-15nm for crest and trough

To further investigate the formation mechanism of the helices, the self-assembled solution was put at a higher temperature to find possible intermediates disassembled from the helical fibrils. Single peptoid strands with a height of 3nm (Fig.10b) were observed after putting the peptoid solution with helical fibers (Fig.10a) at 40°C for two days. The observation of helical fibers and single strands provides evidence for the helices forming through a proposed mechanism that involves the twisting of multistrand ribbons.

Simulation models help to understand the molecular structure of the single strand, as shown in Fig. 10c: amphiphilic peptoids have the propensity to pack with each other through hydrophobic interaction and form a rod structure. To decrease the exposure of hydrophobic groups in water for the rods, peptoids would spontaneously twist so that the polar groups can be distributed around the rod, which is observed as single strands, as shown in Fig. 10b. Further evidence for the formation of the helical fibers remains elusive. One proposed mechanism is the single strands could pack in parallel and twist to helical fibers. as Fig.10 d) showed[31]. Further evidence of helical fibrils with different periodicities is required to prove the hypothesis.

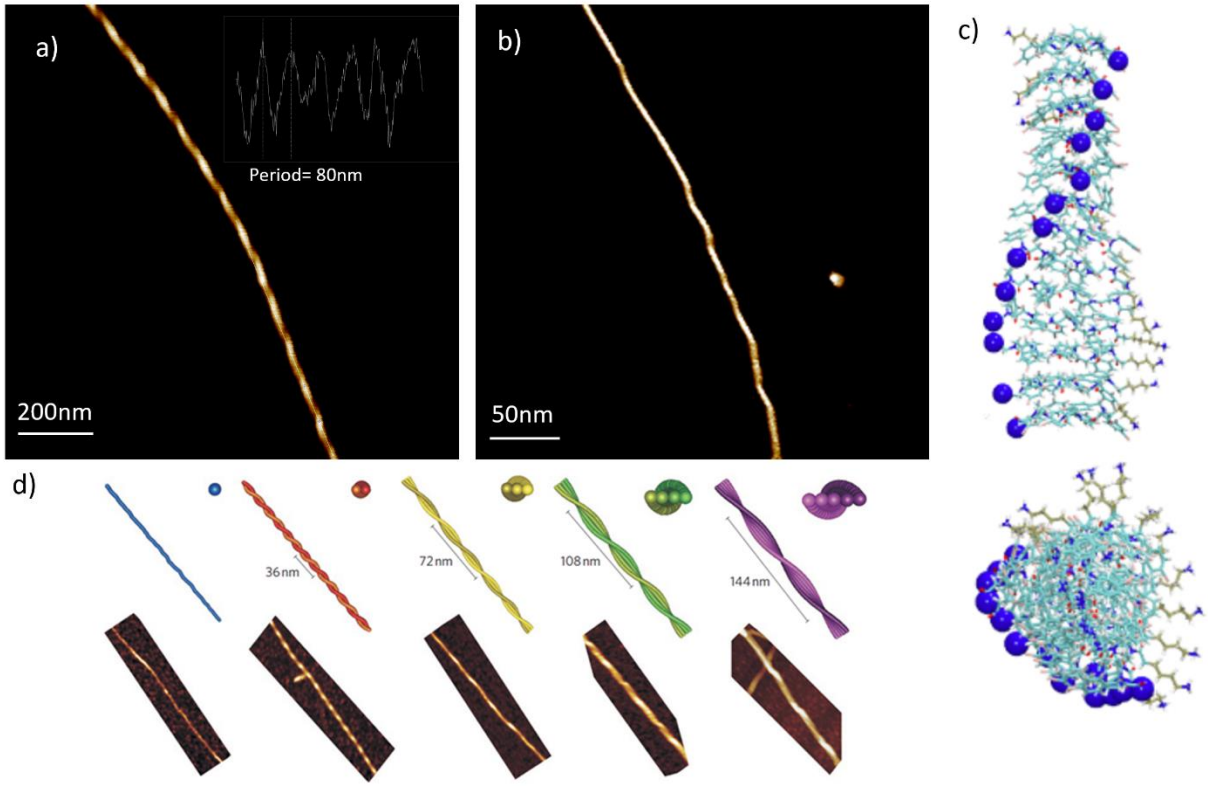

Fig. 10: a) Helical fibers assembled from (NBrpeNBrpm)3Dig with the period of 80nm and the height varied between 10-15nm. b) Single strand with heights of 3nm under 40°C. c) Side and top views of a molecular simulation model of a thermodynamically favored rod-like intermediate during the self-assembly of NBrpe6Nc6. Blue spheres are used to label the C terminal of each peptoid molecule. Similar structure may also account for the single strands observed for (NBrpeNBrpm)3Dig. d) A proposed formation mechanism for amyloid peptide self-assembled helical structures: AFM images and corresponding coarse-grain molecular dynamics reconstructions of helical fibril formation from the twisting of multistranded ribbons[31]. Single strands pack and twist to give helical fibrils.

3.4 Stability test of peptoid nanotube

Since the peptoid self-assembled nanostructures are candidates to induce inorganic material formation, a stability test of the assemblies is required. The templates should remain the self-assembled structures as other conditions like temperature and solution pH changed, which are proved to control the inorganic material formation as well[32-36]. For example, pH variation can be used to mediate the aspect ratio of gold nanoparticles, which is important for their plasmonic properties[37]. Therefore, we also tested the stability of one peptoid nanotube assembled from sequence NBrpm6Nce6 here. It is reported that the nanotube is relatively stable under a wide range of pH conditions[9]. As Fig.11 a) and b) show, the nanotube assembled from peptoid, NBrpm6Nce6 was stable under pH 3.6-8 and performed a height change as pH changes. It is also reported that the tube was stable under a pH of 11.94 for 6 hours. However, when the tube was incubated at a pH of 12 for a longer time, tube morphology was stable after incubation for two days (Fig. 11c) but will change to helical fibers (Fig. 11d) after 5 days and single fiber strands (Fig. 11e) for 10 days and longer. The height decreased from 6nm to 4.5 and 3nm as the morphologies changed from tubes to fibers, which indicated the morphological change was likely to be a disassembly process. Stability test of the peptoid nanotube demonstrate the proper pH range for peptoid self-assemblies' usage. In addition, the helical fibers under basic conditions are also applicable for templates of material growth.

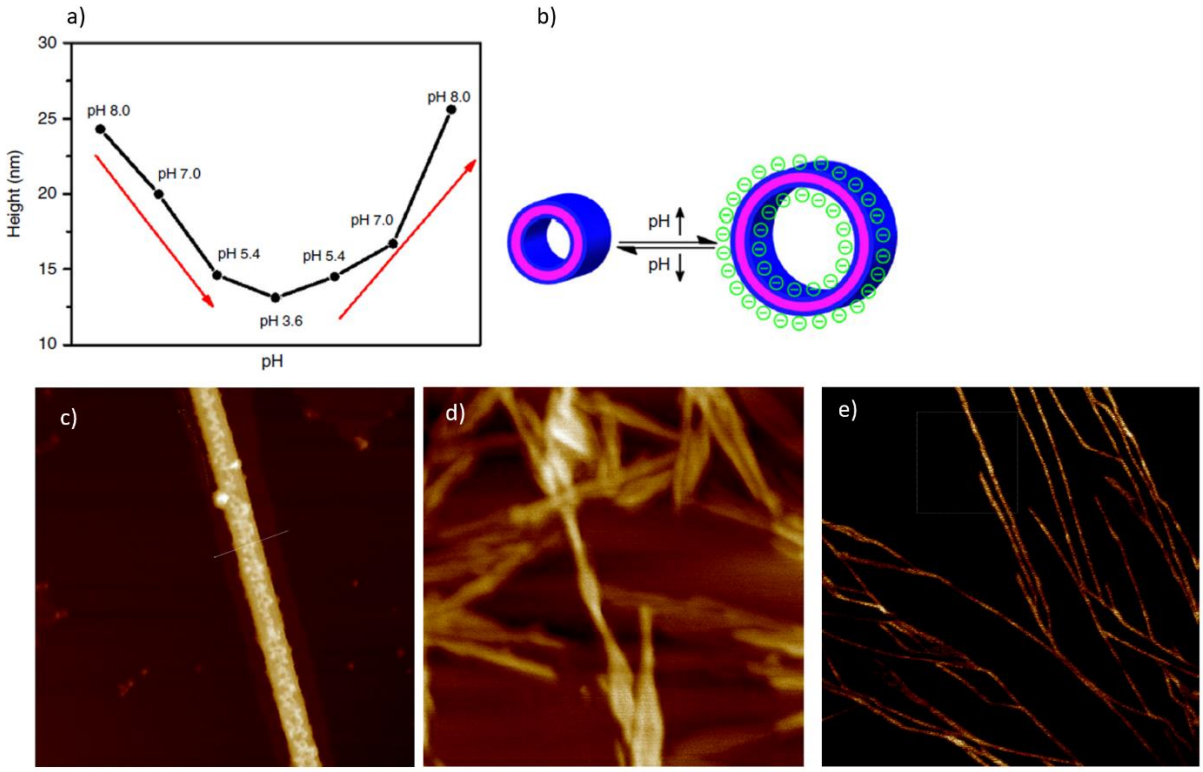

Fig.11: a) pH-responsive height change of peptoid nanotube within the range of 3.6 – 8, where the tube morphology remained. b) Schematic of pH-responsive height change of tubes. Under high pH conditions, hydrophilic carboxyl groups are deprotonated, and the tubes would swell due to increased electrostatic force. c) - e): AFM images of peptoid tube under pH =12, incubating for 2, 5, and 10 days, respectively. Solution pH is mediated through the addition of NaOH solution.

4. Conclusion

In this thesis, we synthesized amphiphilic peptoids comprised of aromatic hydrophobic domains and polar hydrophilic domains to self-assemble into crystallized nanotubes, nanosheets, and nanofibers through an evaporation-induced process. We demonstrated the controlled peptoid self-assembly to different morphologies through variations in either hydrophobic or polar domains in peptoid design. Besides the previously reported conventional nanosheets and nanotubes, we found new morphologies, including nanosheets with stripes as well as helical fibers. In addition, we also demonstrated the stability of one peptoid nanotube under different solution pH and reported a morphological change in this system for high pH and long incubation time. Different morphologies of peptoid self-assemblies can provide possibilities of organized inorganic materials, like metal nanoparticles and quantum dots, with specific 3D arrangements or sophisticated multilayer organic-inorganic hybrid materials. Such materials can be readily adapted to plasmonic, magnetic, optical, and sensing applications.

References

1. Sarikaya, M., et al., *Molecular biomimetics: nanotechnology through biology.* Nature materials, 2003. **2**(9): p. 577-585.
2. Chen, C.-L. and NL. Rosi, *Peptide-Based Methods for the Preparation of Nanostructured Inorganic Materials.* Angewandte Chemie International Edition, 2010. **49**(11): p. 1924-1942.
3. Min, J., et al., *Synthesis of Polylysine/Silica Hybrids through Branched-Polylysine-Mediated Biosilicification.* ACS omega, 2018. **3**(12): p. 17573-17580.
4. Xuan, S. and R.N. Zuckermann, *Diblock copolypeptoids: a review of phase separation, crystallization, self-assembly and biological applications.* Journal of Materials Chemistry B, 2020. **8**(25): p. 5380-5394.
5. Zuckermann, R.N., et al., *Efficient method for the preparation of peptoids [oligo (N-substituted glycines)] by submonomer solid-phase synthesis.* Journal of the American Chemical Society, 1992. **114**(26): p. 10646-10647.
6. Yan, F., et al., *Controlled synthesis of highly-branched plasmonic gold nanoparticles through peptoid engineering.* Nature Communications, 2018. **9**(1): p. 2327.
7. Tigger-Zaborov, H. and G. Maayan, *Aggregation of Ag (0) nanoparticles to unexpected stable chain-like assemblies mediated by 2, 2′-bipyridine decorated peptoids.* Journal of colloid and interface science, 2019. **533**: p. 598-603.
8. Tigger-Zaborov, H. and G. Maayan, *Nanoparticles assemblies on demand: Controlled aggregation of Ag (0) mediated by modified peptoid sequences.* Journal of colloid and interface science, 2017. **508**: p. 56-64.
9. Jin, H., et al., *Designable and dynamic single-walled stiff nanotubes assembled from sequence-defined peptoids.* Nature Communications, 2018. **9**(1): p. 270.
10. Jin, H., et al., *Highly stable and self-repairing membrane-mimetic 2D nanomaterials assembled from lipid-like peptoids.* Nature communications, 2016. **7**(1): p. 1-8.
11. Merrill, N., et al., *Tunable Assembly of Biomimetic Peptoids as Templates to Control Nanostructure Catalytic Activity.* Nanoscale, 2018. **10**.
12. Monahan, M., et al., *Peptoid-directed assembly of CdSe nanoparticles.* Nanoscale, 2021.
13. Zuckermann, R.N., *Peptoid origins.* Peptide Science, 2011. **96**(5): p. 545-555.
14. Lingwood, D. and K. Simons, *Lipid rafts as a membrane-organizing principle.* science, 2010. **327**(5961): p. 46-50.
15. Fletcher, D.A. and R.D. Mullins, *Cell mechanics and the cytoskeleton.* Nature, 2010. **463**(7280): p. 485-492.
16. Shoulders, MD and R.T. Raines, *Collagen structure and stability.* Annual review of biochemistry, 2009. **78**: p. 929-958.
17. Knowles, T.P., M. Vendruscolo, and C.M. Dobson, *The amyloid state and its association with protein misfolding diseases.* Nature reviews Molecular cell biology, 2014. **15**(6): p. 384-396.

18. Rothemund, P.W., *Folding DNA to create nanoscale shapes and patterns.* Nature, 2006. **440**(7082): p. 297-302.
19. Ma, X., et al., *Tuning crystallization pathways through sequence engineering of biomimetic polymers.* Nature materials, 2017. **16**(7): p. 767-774.
20. Ma, J., et al., *Nanoparticle-mediated assembly of peptoid nanosheets functionalized with solid-binding proteins: Designing heterostructures for hierarchy.* Nano Letters, 2021. **21**(4): p. 1636-1642.
21. Yang, W., Q. Yin, and C.-L. Chen, *Designing Sequence-Defined Peptoids for Biomimetic Control over Inorganic Crystallization.* Chemistry of Materials, 2021.
22. Chen, C.-L. and A.M. Beatty, *Guest Inclusion and Structural Dynamics in 2-D Hydrogen-Bonded Metal− Organic Frameworks.* Journal of the American Chemical Society, 2008. **130**(51): p. 17222-17223.
23. Newman, J. and G. Blanchard, *Formation of gold nanoparticles using amine reducing agents.* Langmuir, 2006. **22**(13): p. 5882-5887.
24. Amari, H., et al., *In situ synthesis of silver nanoparticles on densely amine‐functionalized polystyrene: Highly active nanocomposite catalyst for the reduction of methylene blue.* Polymers for Advanced Technologies, 2019. **30**(2): p. 320-328.
25. Ding, B., et al., *Gold nanoparticle self-similar chain structure organized by DNA origami.* Journal of the American Chemical Society, 2010. **132**(10): p. 3248-3249.
26. Pazos, E., et al., *Nucleation and growth of ordered arrays of silver nanoparticles on peptide nanofibers: hybrid nanostructures with antimicrobial properties.* Journal of the American Chemical Society, 2016. **138**(17): p. 5507-5510.
27. Fu, X., et al., *Assemblies of metal nanoparticles and Self‐Assembled peptide Fibrils—Formation of double helical and Single‐Chain arrays of metal nanoparticles.* Advanced Materials, 2003. **15**(11): p. 902-906.
28. Cheng, J., et al., *GoldHelix: Gold nanoparticles forming 3D helical superstructures with controlled morphology and strong chiroptical property.* ACS nano, 2017. **11**(4): p. 3806-3818.
29. Chen, C.-L., P. Zhang, and N.L. Rosi, *A new peptide-based method for the design and synthesis of nanoparticle superstructures: construction of highly ordered gold nanoparticle double helices.* Journal of the American Chemical Society, 2008. **130**(41): p. 13555-13557.
30. Mokashi‐Punekar, S., et al., *Construction of Chiral, Helical Nanoparticle Superstructures: Progress and Prospects.* Advanced Materials, 2019: p. 1905975.
31. Adamcik, J., et al., *Understanding amyloid aggregation by statistical analysis of atomic force microscopy images.* Nature nanotechnology, 2010. **5**(6): p. 423-428.
32. Kimling, J., et al., *Turkevich method for gold nanoparticle synthesis revisited.* The Journal of Physical Chemistry B, 2006. **110**(32): p. 15700-15707.
33. Mody, V.V., et al., *Introduction to metallic nanoparticles.* Journal of Pharmacy and Bioallied Sciences, 2010. **2**(4): p. 282.
34. Pandey, R.B., et al., *Adsorption of peptides (A3, Flg, Pd2, Pd4) on gold and palladium surfaces by a coarse-grained Monte Carlo simulation.* Physical Chemistry Chemical Physics, 2009. **11**(12): p. 1989-2001.
35. Li, C., et al., *Facile synthesis of concentrated gold nanoparticles with low size-distribution in water: temperature and pH controls.* Nanoscale research letters, 2011. **6**(1): p. 1-10.

36. Wang, H., et al., *Preparation of silver nanoparticles by chemical reduction method.* Colloids and Surfaces A: Physicochemical and Engineering Aspects, 2005. **256**(2-3): p. 111-115.
37. Wei, Q., J. Ji, and J. Shen, *PH controlled synthesis of high aspect-ratio gold nanorods.* Journal of nanoscience and nanotechnology, 2008. **8**(11): p. 5708-5714.